Women in Aerospace

University of Illinois at Urbana-Champaign

Team Mentor: Jonathan Sivier

Faculty Adviser: Diane Jeffers (dejeffer@illinois.edu)

Team Lead: Alexandra Bacula (bacula2@illinois.edu)

Katherine Carroll

Ian Charter

Melanie Ciancio

Sara Kochanski

Sara Legg

Christopher Lorenz

Lui Suzuki

March 18, 2016

TABLE OF CONTENTS

TABLE OF FIGURES

TABLE OF TABLES

Executive Summary

The rocket and active drag system were designed with both effectiveness and simplicity in mind in order to get the most streamlined design, while still having exceptional performance both in flight and in the results of the active drag. The rocket will be made primarily out of Blue Tube for the main body, a plastic nose cone, and fiberglass aerodynamic fins. These materials were chosen for their low weight and high strength, leading to a reliable performance. The cost of these materials also made them a realistic choice for the team.

The active drag system will consist of a linear actuator, spur and rack gears, and two active drag fins made of fiberglass. During the flight in which the active drag is engaged, the actuator will rise and turn the plywood fins 90 degrees in order to create more drag and slow down the rocket. The materials for the active drag were also chosen for their reliability and high performance, while still being realistic in terms of cost. The goals of the team for this competition are to design and build a working system that meets the competition requirements, is unique and innovative, is reliable and performs to a high standard, and to also obtain useful data from the flights in order to analyze and evaluate the performance of the system and learn from the strengths and flaws of the design.

1. Mechanical and Electrical Design

1.1 Overall Dimensional Specifications

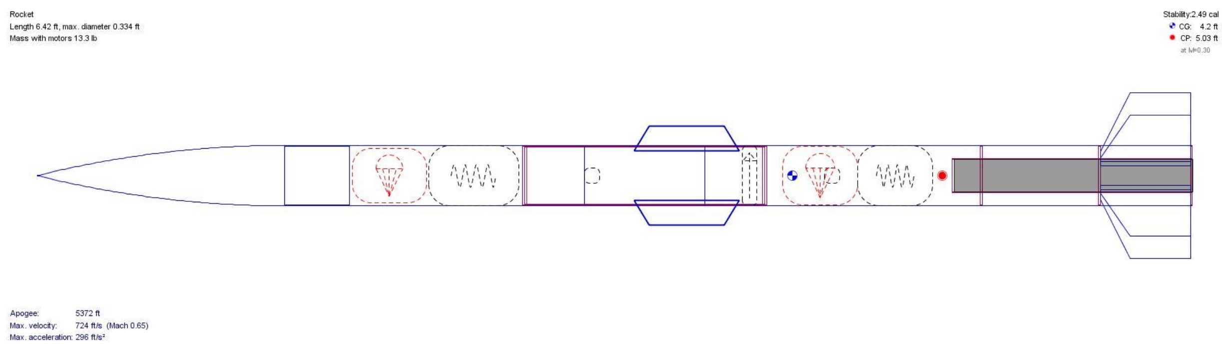

Figure 1. OpenRocket Diagram of Rocket Before Motor Burnout

The total length of the rocket is 6.42 ft with an outer diameter of 4 in. It consists of a nose cone upper airframe section, coupler section, and booster section. The total weight of the rocket, including the full weight of the motor, is 13.3 lbs. The center of pressure is denoted by a red dot on Figure 1 and is located 5.03 ft from the tip of the nose cone, or 1.39 ft from the base. The center of gravity is denoted by a blue and white dot on Figure 1. It is located 4.20 ft from the tip of the nose cone, or 2.22 ft from the base before the motor has burned out. Once the motor burnout occurs, the center of gravity moves to 3.92 ft from the tip of the nose cone, or 2.5 ft from the base. A plot showing the location of the center of gravity as the motor burns can be seen in Figure 2.

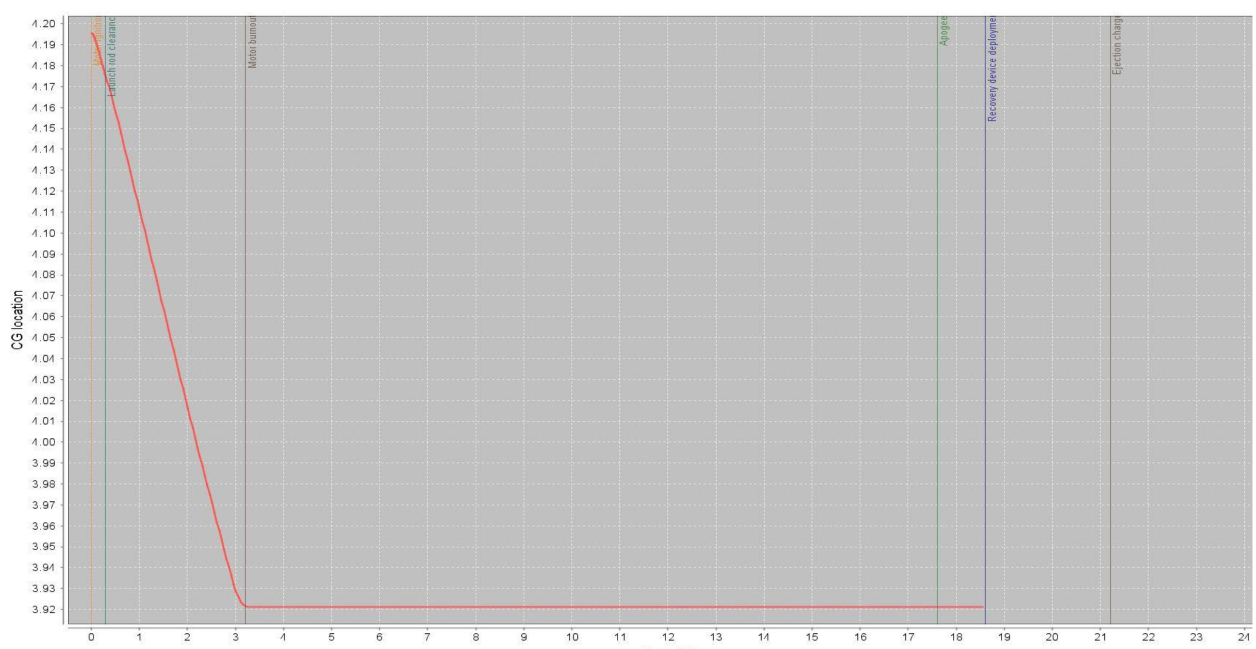

Figure 2. Center of Gravity Location from the Tip of Nose Cone

1.2 Rocket Airframe Design Features

1.2.1 Motor Selection and Propulsion System Specifications

The motor was chosen to maximize the ability to achieve competition goals, while simultaneously minimizing the possibility of failure for the rocket. Only rocket motors of class "K" (1280-2560 Ns) were studied due to competition rules and similarly, due to the motor vendor for the launch, only Cesaroni Technology Incorporated (CTI) motors were considered. The rocket diameter was chosen to be 4 in. based on initial analysis, so the team limited the diameter of the chosen motors to below 75 mm. A final competition constraint is that a motor ejection charge must act as a backup for the drogue parachute. If this ejection occurs before apogee, the active drag system cannot be scored. Given these constraints, the team eliminated plugged rocket motors as well as any whose charge would ignite prior to apogee.

From these parameters, a set of motors was identified that allowed the rocket to reach at or near the required 5,000 ft AGL altitude to achieve maximum points in the competition. All of these motors were checked to ensure they would allow the rocket to exceed a standard rail exit velocity of 65.6 ft/s (20 m/s) for the 8 ft competition rail and the required 45 ft/s at the 6 ft point. These rocket motors are summarized in Table 1 below.

Table 1. Motor data comparison.

Motor	Altitude (ft)	Rail Exit Velocity (ft/s)	Rail Velocity at 6 ft (ft/s)	Maximum Velocity (ft/s)	Maximum Acceleration (ft/s^2)	Motor Burn Time (s)
K500	5372	66.1	57.7	724	296	3.16
K2045 VMax	4921	137	119	804	1246	.709
K360	4394	54	46.6	599	201	3.48

As can be seen above, the K360 did not meet either of the velocity requirements while on the launch rail, so it was eliminated. In choosing a motor within this range, several secondary concerns were taken into account. Motors with short burn times were considered preferable, as they allow the active drag system more time to slow the ascent of the rocket. At the same time, motors that lead to lower launch accelerations were desirable to decrease the loading on internal and external components. Directly related to this, low burnout velocities will lead to a decrease in force on the fins, especially by avoiding transonic effects (Mach number greater than about 0.7). These attributes are in direct competition, as a decrease in burn time typically leads to an increase in acceleration and burnout velocity.

Ultimately, the team chose the Cesaroni K500 as it will provide the best trade between burn time and loading for the rocket. The short burn time of 3.16 s will allow the active drag system an estimated 14.44 s window of operation. While this burn time is longer than that of the K2045 VMax, both the main fins and the active drag fins would not be able to withstand the maximum acceleration of the K2045 VMax, and the velocities of that motor would be transsonic. The team calculated the loading on the fins using a simplified drag model as

$$D = C_d \times \frac{V^2 \times \rho}{2} \times A \tag{1}$$

in which $D$is the drag force, C_d is the drag coefficient of the fins, V is the velocity of the rocket, ρ is the density of air, and A is the area of the fins. The calculated maximum drag force on each fin occurs at peak velocity and is 91.752 N using the K500. The calculated maximum drag force on each fin occurs at peak velocity and is 113.457 N using the K2045 VMax.

The Cesaroni K500 is a reloadable motor that is 54 mm (2.13 in.) in diameter and 404 mm (15.91 in.) in length. It has a burn time of 3.16 s and an ejection charge delay of 18 s. It has an average thrust of 502 N and a maximum thrust of 595 N occurring at 0.50 s. The thrust curve can be seen below in Figure 3. The total impulse is 1587 Ns. The launch mass of the motor is 3.25 lbs and the mass after burnout is 1.26 lbs.

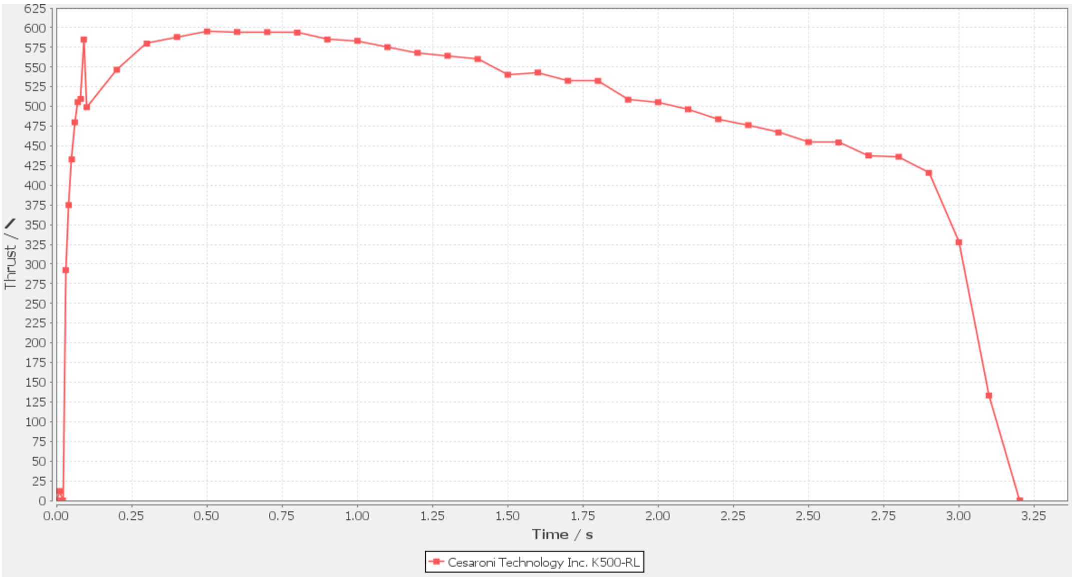

Figure 3. Cesaroni K500 Thrust Curve

1.2.2 Upper Airframe

The upper airframe consists of the nose cone, a Blue Tube section, the main parachute, shock cords, quick links, and parachute protectors. The nose cone has an ogive profile, a shoulder length of 3.25 in., an outer diameter of 4 in., and is 16.5 in. long. It is made out of polypropylene plastic and weighs 0.657 lbs (298.1 g) alone, but will have an extra ballast mass of 8.16 g (0.018 lbs) added. This weight helps to increase the stability of the rocket to ensure that it remains at a safe stability margin throughout flight. The Blue Tube section connected to the nose cone is 1.67 ft in length and weighs 0.666 lbs. This Blue Tube section holds the main parachute and its accessories. At the base of the upper airframe will be an eye bolt to attach the main parachute. On the bulkhead separating the upper airframe and the coupler will be an ejection charge to deploy the main parachute. In regards to the material of the upper airframe and the vehicle's body in general, the team has chosen to use Blue Tube as it is an inexpensive material that is also relatively strong. Carbon fiber would be the best option as it is light in mass and stronger than both fiberglass and Blue Tube, however it can be hazardous to work with and is significantly more expensive. While fiberglass is also stronger than Blue Tube, it is more expensive and is twice as heavy. An additional reason the team decided to use Blue Tube is that it is rated high enough to withstand the loads it will encounter throughout the mission. Blue Tube is also shatterproof which greatly increases the reusability of the rocket.

1.2.3 Coupler

The coupler section consists of two 8 in. sections of Blue Tube joined together by epoxy, totaling 1.33 ft in length. Inside is the active drag system, avionics, and bulkheads. There is a Blue Tube switchband centered on the outside of the coupler measuring 8 in. in length with an outer diameter of 4 in. and a thickness of 0.007 in., to create space between the upper airframe and booster section while reinforcing the connection point of the two coupler sections and adding extra strength around the active drag system. The two bulkheads at the end of the coupler are made out of 0.25 in. thick plywood, have an outer diameter of 3.733 in., and each weigh 0.115 lbs. These will separate the active drag and avionics, as well as serving as an attachment point for the eye bolts to attach the main and drogue parachutes.

1.2.4 Booster Airframe

The booster airframe consists of a Blue Tube section with a 4 in. diameter measuring 1.67 ft in length. Inside the airframe is the drogue parachute and its accessories. At the top of the booster section, on the outer side of the coupler bulkhead, will be the eye bolt to attach the drogue as well as the drogue ejection charge. In addition, the booster airframe will house the motor, fixed with the motor mount and motor retainer, which will be held in place by three centering rings made of plywood as well as an aft enclosure. On the outside of the booster airframe are four fiberglass fins made out of 0.125 in. thick fiberglass. They will be spaced equally around the rocket, each with a span of 4.8 in. measuring 4 in. at the tip and 6 in. at the root. The fins will be epoxied to the motor mount tube inside of the body tube for additional support. Along the outside of the airframe will be two 1515 rail buttons made out of Delrin-plastic with a length of 0.68 in. and an outer diameter of 0.63 in. Rail buttons will ensure that the rocket leaves the launch rail in the desired direction.

1.2.5 Recovery System

The recovery system of the vehicle will be comprised of an 18 in. drogue parachute stored in the booster section and a 48 in. main parachute housed in the upper airframe. Other components included in the recovery system consist of tubular nylon shock cords, parachute protectors, quick links, eye bolts, shear pins, and an ejection charge. The sizes of the drogue and the main were determined through various simulations in OpenRocket and from the experience of the team mentor. The 18 in. drogue parachute is made out of ripstop nylon, weighs 0.041 lbs, and has a drag coefficient of 0.80. The 48 in. main parachute is made out of ripstop nylon, weighs 0.187 lbs, and has a drag coefficient of 1.80. The main parachute is attached to a 15 ft tubular nylon shock cord weighing 0.161 lbs. The shock cord is then attached to 4 quicklinks, which are hooked onto an eye bolt. The eye bolt will be screwed into the coupler and secured by washers and a nut. The ejection charges are located on the sides of the bulkheads facing out of the coupler. The ejection charge for the drogue will have 1 g of black powder, while the ejection charge for the main parachute will have 2 g of black powder. The amount of black powder was determined using an online black powder ejection charge calculator which took into account the diameter and length of the section in which the parachute is stowed, as well as the pressure needed for successful parachute ejection, which is typically 10 to 15 PSI for a 4 in. diameter rocket.

1.3 Electronic and Payload Design Features

1.3.1 Active Drag System

The active drag system consists of two rotating fins located at a distance of 27 in. from the base of the rocket. The fins will have a trapezoidal shape with a root chord of 7 in. and a tip chord of 5 in. They will be 2 in. wide and constructed out of plywood that is 0.25 in. thick. The rotation point of the fins is located 3 in. below the center of gravity of the rocket after the motor has burned out. The location of the active drag system was chosen such that it will coincide with the center of gravity of the rocket in order to maintain stability. A CAD model of the active drag system can be seen in Figure 4.

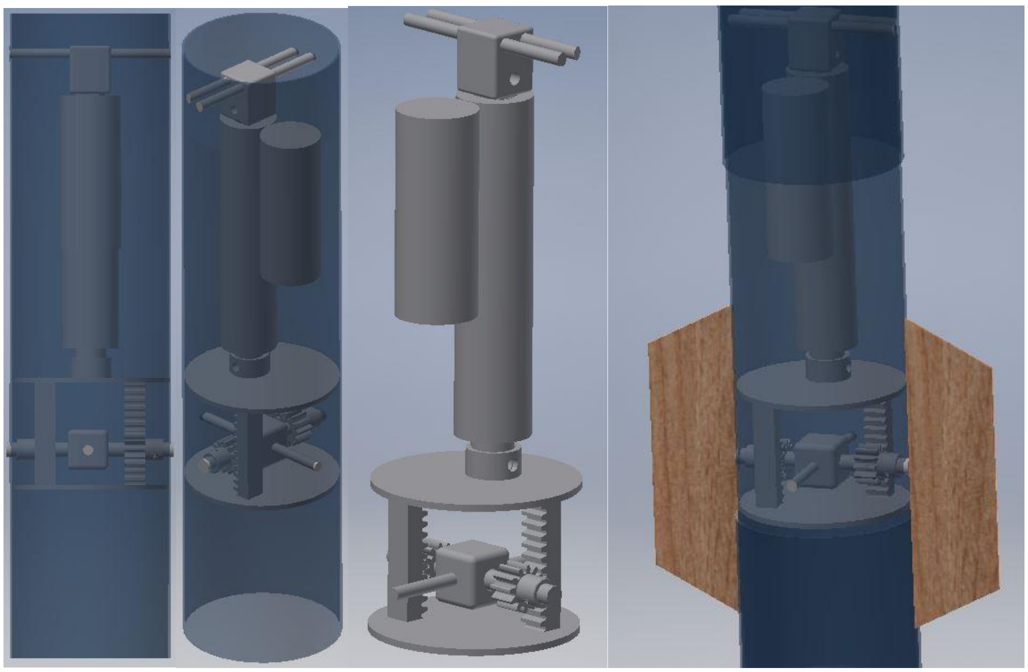

Figure 4. Four Views of the CAD Model of the Active Drag System

When disengaged, the fins are stowed such that they run parallel to the rocket body in order to reduce drag as seen in the far right view in Figure 4. The drag system will be activated after motor burnout and will be deactivated and returned to initial configuration before apogee. Upon activation, the fins will pivot 90° on their center axis becoming aligned perpendicular to the body tube. This will increase the surface area and, therefore, the drag on the rocket. The fins and attachments will be sturdy enough that they will not fracture or tear off the rocket body when activated.

Each fin of the active drag system will be attached to a rod running into the rocket and attached along the centerline of the rocket to a mounting block. Each rod will pass through a spur gear that will run along a gear rack. The gear racks will be on opposite sides for each gear so that the gears and fins will turn in opposing directions. This will prevent the rocket from drifting laterally and, more importantly, from tumbling about the lateral axis as the fins rotate. By turning the fins in opposite directions, stability will be maintained and the rocket will not break apart as the active drag is applied. The two gear racks will be attached to mounting plates on both the top and bottom of the racks. The bottom mounting plate will be fixed to the top of a 3 in. stroke linear actuator.

As the actuator moves vertically the gear racks will move as well and force the gears to turn which in turn rotates the fins. The actuator will be powered by a 12V battery and a motor controller that is used to supply the proper amount of power to the actuator. Movement will be triggered by an Arduino that will be programmed to send speed and direction information to the motor controller. The motor controller will then provide the necessary power to the screw drive of the actuator to raise or lower the shaft as desired.

1.3.2 Avionics

The avionics system will be included in the coupler section of the body tube. The avionics bay will be in the bottom half of the coupler section taking up approximately 4.65 in length. It will be separated from the bottom booster section and upper active drag component with a bulkhead.

Components of the avionic system include two threaded rods and a plywood sheet for the avionics bay, two altimeters, two 9V, batteries, two switches, three terminal blocks, and wires. The avionics bay will be the platform on which all of the avionics will be secured on and will be a rectangular piece of plywood. It will have two rows of small 3D printed tubular guides epoxied to the plywood a few inches apart each. The threaded rod will be passed through these guides to attach onto the avionics bay and the bulkheads that will go on the end of the avionics coupler section.

On the avionics bay, two altimeters (most likely stratologgers) will be screwed on and two 9V battery holders will either be epoxied or screwed on. One stratologger will fire the main charge on the main and drogue parachute. The second stratologger will fire the backup charge for the main parachute. No backup from the stratologger is needed for the drogue parachute because the motor charge will serve as the backup. Wires will be connecting the stratologgers to the charges, battery, and switches.

The stratologgers will have independent switches to arm and disarm them. The rotary switches will be passed through a hole in the body tube of the coupler section and will be screwed in with a nut. One switch will control the main charge stratologger while the other will control the backup charge stratologger. Each switch will be clearly labeled as to which stratologger it controls, which position is on and which position is off.

Wires from the ports of the stratologger named drogue and main will be led through the coupler and bulkhead to the outside of the bulkhead. They will then be connected to the terminal block which is connected to the black powder charges on the other end. Using these terminal blocks makes assembly of the coupler and charges easier.

There will also be a pressure sensor on the avionics bay. The pressure sensor will be screwed on similar to the stratologgers. It will be used to take measurements of the coefficient of drag during flight. This data will be used post flight to create a model of the active drag system.

Additionally, there will be a small camera on the bay aimed at the active drag system. This camera will allow the operation of the active drag to be filmed, which is useful data for the team for many reasons. With the footage the team will be able to see the movement of the active drag, which allows for better evaluation of the performance and allows for easier troubleshooting if something were to go wrong in the operation of the system. The footage also provides comparison points with the data. The data gathered from the pressure sensor can be compared to the video to see what physically changed during active drag operation to affect the coefficient of drag.

1.4 Construction Process

The construction of the rocket will be broken down into various sections that will take place throughout the second half of the spring semester. All parts necessary for manufacturing and assembly were ordered in early February and were delivered in mid March. Construction of each section is scheduled to begin on March 29th. Team members will work in the pairs so that no member is working alone in the student workstations for safety reasons. This will also help to reduce potential mistakes that could occur during the building process.

Upon receipt, all parts have been inventoried, inspected, weighed, cleaned, and labeled. Before permanently attaching any components, the rocket will be assembled as fully as possible to make sure that each manufactured part fits the correct dimensions. General construction practices will include marking all hole locations, confirming hole and insert sizes, and reaffirm locations before drilling or fastening with epoxy. Basic construction tools and supplies include but are not limited to an X-Acto knife, a drill and bits, a Dremel tool, a soldering iron and a palm sander. A high strength epoxy will be used for bonding major areas of the flight vehicle. Surfaces that will have epoxy applied will be sanded with 60 grit or coarser sandpaper and will be later cleaned with rubbing alcohol. The amount of epoxy applied will be determined by the structural integrity and consequential drag effects while in flight. Hazards associated with exposure to epoxy have been addressed and actions taken to mitigate risk are noted in Section 1.6.

Construction of the rocket will begin with the motor mount. Three centering rings made of 0.25 in. plywood will be used for structural support and ease of alignment. The location of the centering rings will be marked on the motor mount and body tube in three different locations: the top ring slightly below the top of the motor mount tube, the middle ring aligned with the top of the fins, and the bottom ring aligning the retainer with the bottom of the rocket. Motor retention will be ensured by an Aero Pack 54mm Motor Retainer constrained at the extreme aft end of the rocket.

Next, rail button positions will be marked on the airframe and attached before the motor mount is fixed inside of the rocket. To secure the rail buttons, T-nut interfaces will be created on the inside of the rocket. The interfaces will consist of a T-nut inserted into a block of plywood and will be mounted to the top and bottom centering rings. Next, the inside of the booster airframe and the fin slots will be sanded. Epoxy will be applied to the top of the aft centering ring, through a hole for the top ring, and through a fin slot for the middle ring. The motor mount will be inserted into its marked location in the booster airframe at a later time.

Another component of the construction process is assembling the avionics bay. All electronics will be carefully soldered to assigned locations on the avionics sled and appropriate electrical hardware will be used to make sure that no wires are left exposed. Threaded rod rails will be attached to the bulkhead and run the length of the avionics bay to act as guide rails for the avionics sled as it is inserted into the airframe. The avionics sled will have two hollow tubes attached to the sides lengthwise. The threaded rods are able to slide into the hollow tubes, securing the avionics bay in place. The bulkheads of the avionics bay will also have charge cups, terminal blocks, and eyebolts for parachutes attached to them.

The trapezoidal fins will be carefully constructed out of 0.125 in. fiberglass and will be in a through-the-wall configuration. Upon construction, fin alignment will be ensured through the use of a simple jig consisting of slots placed 90° apart. When affixing the fins, a generous amount of epoxy will be applied between the fins and the body tube for support, making sure that no residue is left to create undesirable drag consequences. Internal fillets for the fins will assure that the fins fit tight to the motor mount tube and that the centering rings fit snug to the top and bottom of the fins.

The active drag system of the rocket will be constructed by first mounting bars at the stationary top of the linear actuator to the body tube walls. Next, the upper mounting plate, with the two gear racks already attached, will be fixed to the moving head of the linear actuator. Then gears will be attached to the rods for the drag fins and rods will be fixed to the mounting block followed by these components being situated within the rocket. The system will be completed by fixing the bottom mounting plate to the gear racks to close and secure the entire system. Construction techniques are subject to change as the team approaches obstacles in the manufacturing process.

Verification of the vehicle construction will be accomplished as components are completed by experienced team members and the team mentor. These individuals will inspect all connections and other construction features to ensure that the manufacturing process proceeds as planned and provides for sufficient structural integrity. Additionally, each time a component is completed, its integration with other completed parts will be tested. Inspecting components as they are completed will allow the team to catch any errors or defects as early as possible, and resolve the problems as they arise. The building process will conclude with priming and painting the exterior for aesthetic appeal and drilling pressure relief holes in the airframe to allow pressure to equalize in flight.

1.5 Structural Analysis of Scratch Built Parts

The majority of the rocket is scratch built, so it is integral to the rocket that the components are structurally sound. The main body tube will be put under many forces during flight and recovery so the team chose to use Blue Tube due to its durability and high strength. Blue Tube is shatterproof, eliminating the worry of the body tube breaking and splintering under stress or impact. Team members have flown many rockets with great success using Blue Tube as the main body tube. The aerodynamic and active drag fins will be made of fiberglass due to its high strength. While they are heavier, the fiberglass will be able to withstand the forces of flight and the impact of landing most reliably. The fins are attached through the body tube to the motor mount, adding extra assurance that they will be able to withstand flight and landing conditions. The epoxy used to hold on the fins is strong enough to secure the fins to the body tube, while being elastic enough to bend slightly as force is put on the fins during flight. Epoxy will also be used to hold together the coupler. The epoxy will create a strong bond joining the two sections of coupler and will be able to withstand the forces of launch and landing. The avionics sled will be manufactured out of plywood due to its low weight and relatively high strength. The plywood sled will be sturdy enough to hold all the avionics securely in place, while still being light weight.

1.6 Risk Mitigation Analysis

There are many risks that come with constructing a rocket. To maintain a safe working environment, the team has addressed these risks. In Table 2 on the following page, possible risks are listed, as well as how the team plans to prevent the risk.

Table 2. Risk mitigation.

Possible Risk	**Mitigation Solution**
Skin contact with epoxy	Wear gloves at all times when handling epoxy
Power tool accidents	All team members will be trained on power tools by experienced instructors--safety equipment such as safety glasses and earplugs will be worn throughout build process
Inhaling fiberglass	Masks will be worn during the cutting of fiberglass
Inhaling epoxy fumes	Use proper ventilation in student workspace
Black powder explosion	Black powder, along with all other explosives, will be stored very carefully according to their safety instructions
Electrical Shock	All wiring will be thoroughly checked and tested to ensure the connections are correct before supplying power

2. Predicted Performance

2.1 Launch Analysis

OpenRocket was used to simulate the rocket launch performance with the active drag system disengaged. The simulation was run with the rocket launching off an 8 ft launch rail vertically at 0°. The rail velocity at 6 ft will be 57.7 ft/s, exceeding the required 45 ft/s. The rocket will clear the launch rail at 0.29 s with a rail exit velocity safely above 65.6 ft/s at 66.1 ft/s, a vertical acceleration of 281.5 ft/s^2, and a stability margin of 1.958. At 3.085 s, shortly before motor burnout, the rocket will reach its peak velocity of 724 ft/s. Motor burnout will occur at 3.22 s, at which time the rocket will be at an altitude of 1321.75 ft, a vertical velocity of 704.5 ft/s, a vertical acceleration of -113.7 ft/s^2, and a stability margin of 3.406.

A custom simulation program was used to simulate the rocket launch performance with the active drag engaged. The simulation was run with the rocket launching off an 8 ft launch rail vertically at 0°. The anticipated performance will be the same for both flights with active drag engaged and disengaged because the active drag will not be engaged until after motor burnout and will be in the same stowed position during launch for both flights. The values obtained from this simulation for launch simply serve as a comparison between the OpenRocket simulation and the custom simulation. For the custom simulation, the rail velocity at 6 ft will be 57.65 ft/s. The rocket will clear the launch rail at .29 s with a rail exit velocity of 64.85 ft/s. Shortly before motor burnout, at 3.101 s the rocket will reach its peak velocity of 735.78 ft/s. Motor burnout will occur at 3.21 s, at which time the rocket will be at an altitude of 1330 ft and vertical velocity of 727.8 ft/s.

2.2 Flight Analysis

2.2.1 Estimated Maximum Altitude

The estimated maximum altitude of the rocket was simulated via OpenRocket and a custom simulation program created by the team. These simulations agree very well with each other, giving the team confidence in the reliability of the program. Members of the team have used OpenRocket in the past in many mid and high powered rocketry flights with excellent results. The simulations have routinely overshot the actual altitude by about 5% based on data from past flights, so a slightly lower apogee is expected in flight. Using the OpenRocket simulation, the rocket is expected to reach 5372 ft at a time of 17.61 s. The custom simulation predicts an altitude of 5374.56 ft. A plot with the OpenRocket simulation with event markers can be seen in Figure 5, and plot with both simulation programs' altitude versus time data can be seen in Figure 6.

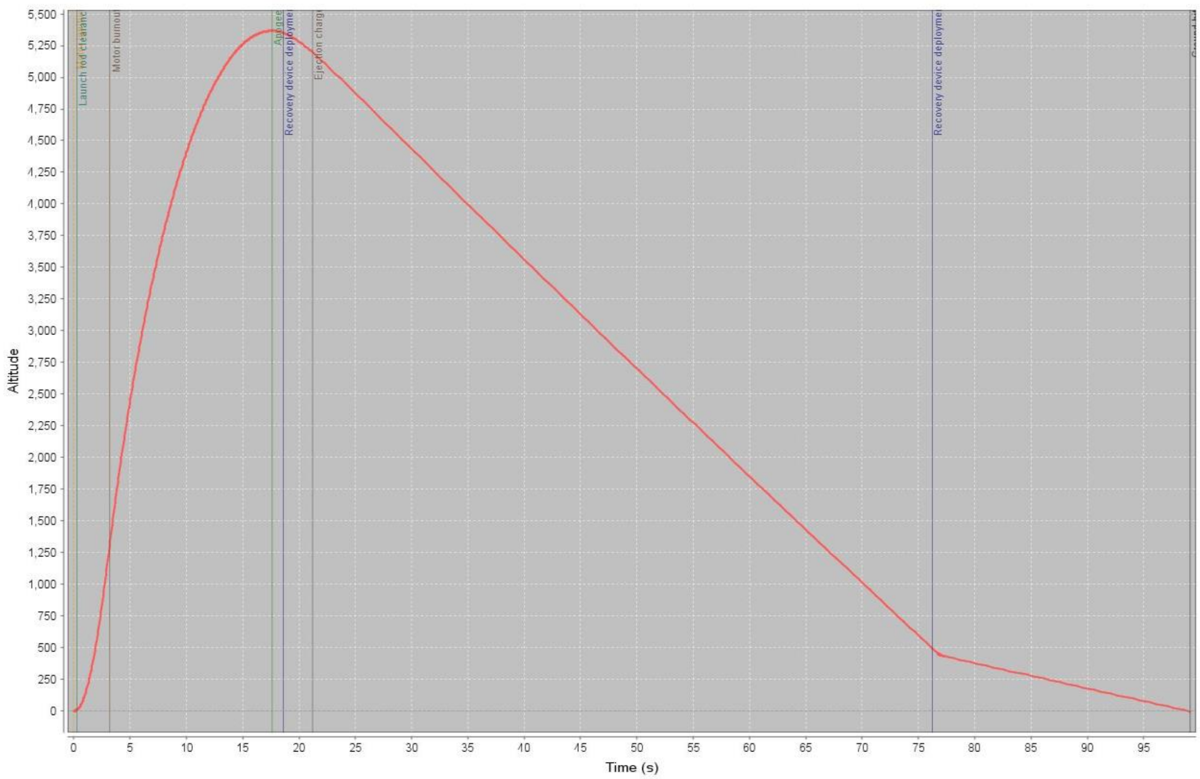

Figure 5. OpenRocket Altitude Simulation, Active Drag Stowed

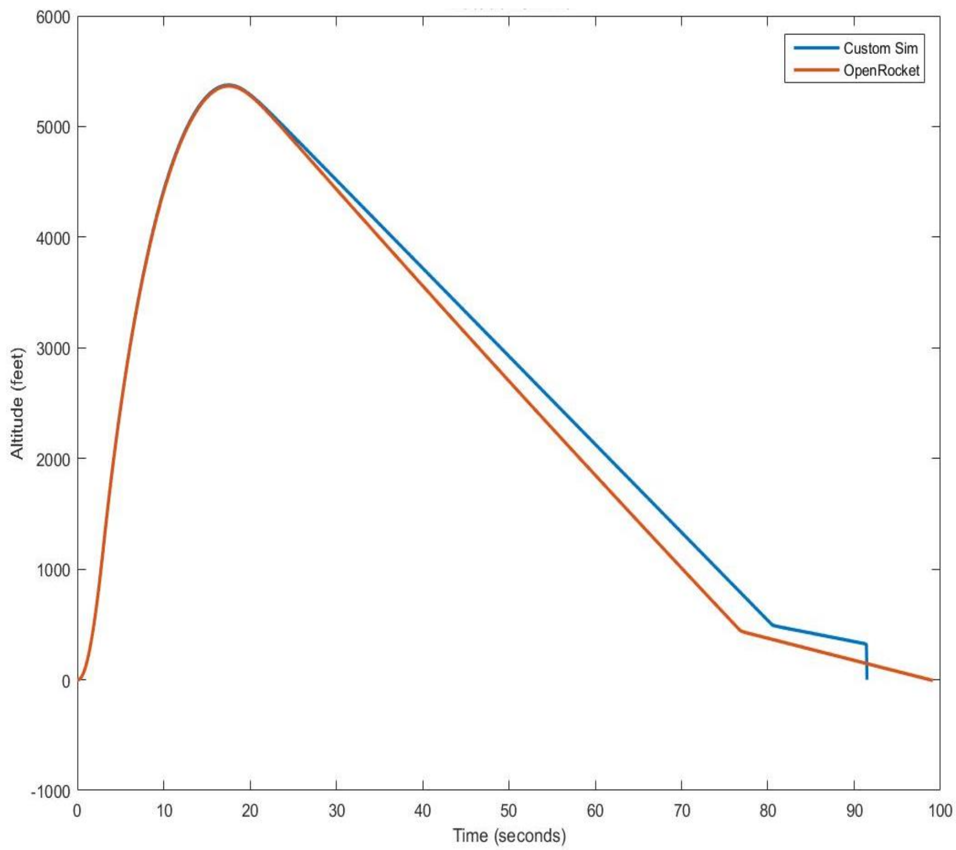

Figure 6. Predicted Altitude, Active Drag Stowed

Unfortunately, OpenRocket does not have the capabilities to accurately model active drag, so the team will rely on the custom simulator to accurately predict its flight. This simulation will be compared to the data gathered from the rocket's test flight and verified to ensure its accuracy. The custom simulation currently has the rocket reaching an altitude of 4000.943 ft. A plot of the altitude versus time for the rocket with the active drag system enabled can be seen in Figure 7.

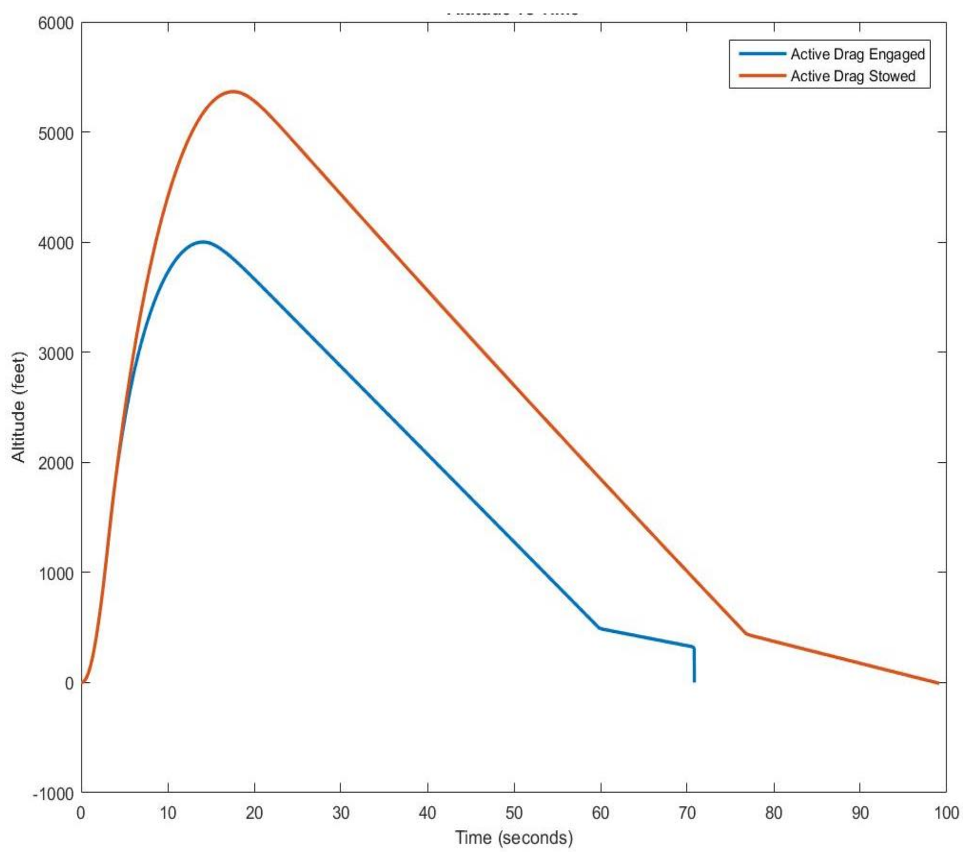

Figure 7. Predicted Altitude, Active Drag Engaged

2.2.2 Estimated Peak Velocity

The estimated peak velocity was also simulated using both OpenRocket and the custom simulation program. OpenRocket works well to model the peak velocity during the flight without the active drag being utilized. The peak velocity as shown by the OpenRocket simulations is 724 ft/s and is achieved near motor burnout as expected. The plot of this simulation can be seen below in Figure 8. The custom simulation shows a peak velocity of 724.02 ft/s during the flight where the active drag is stowed. The plot of this simulation can be seen in Figure 9. When the active drag is engaged, as shown in Figure 10, the peak velocity turns out slightly higher at 735.79 ft/s.

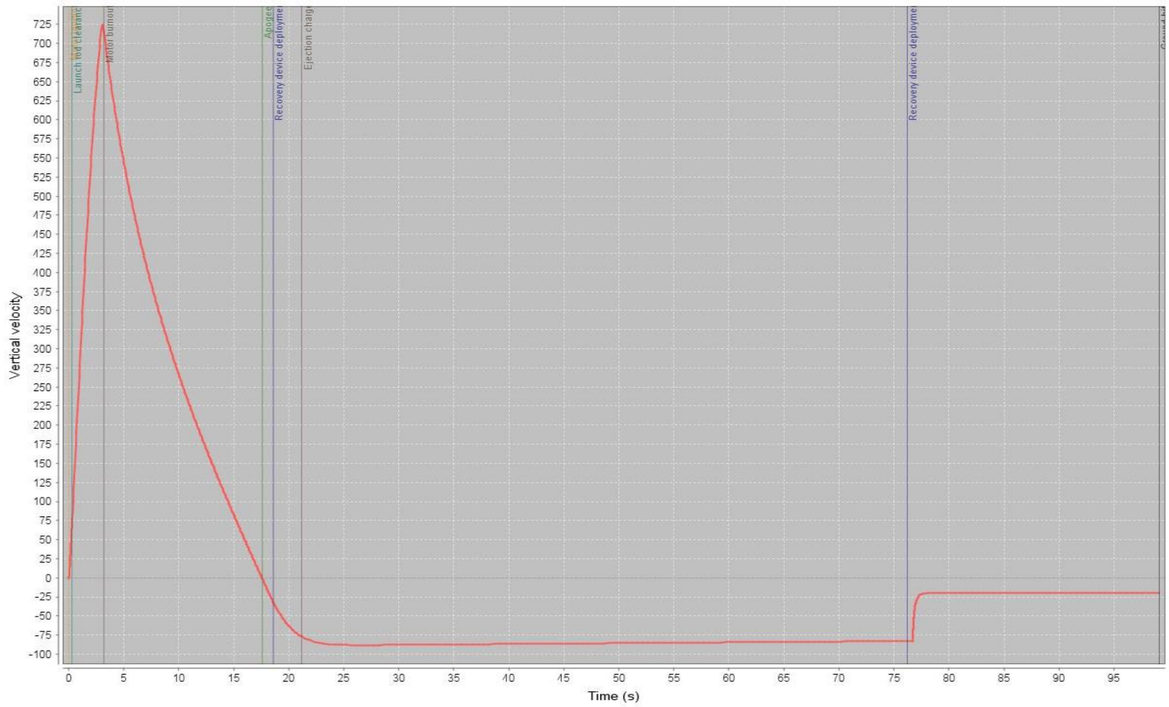

Figure 8. Open Rocket Velocity Simulation, Active Drag Stowed

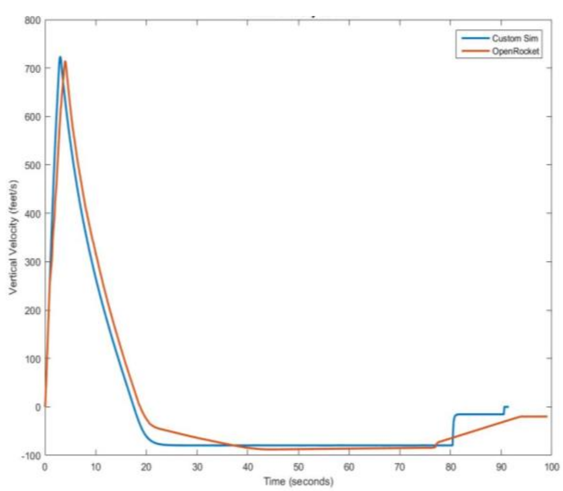

Figure 9. Predicted Vertical Velocity with Active Drag Stowed

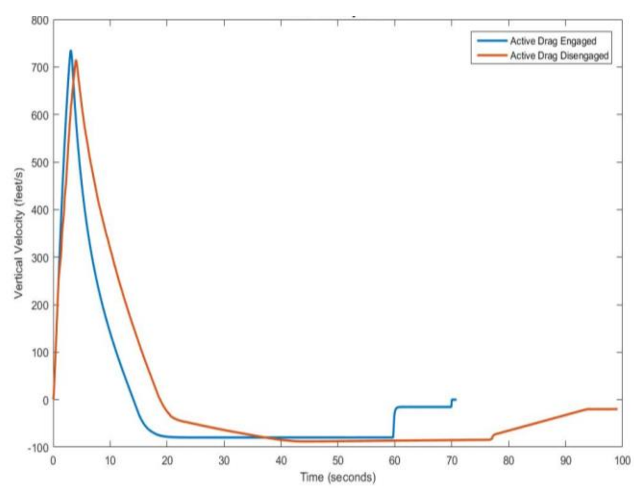

Figure 10. Predicted Vertical Velocity with Active Drag Engaged

2.2.3 Estimated Drag Coefficient

Similar to the peak velocity estimations described in the previous section, the drag coefficient was calculated using both OpenRocket and the custom simulation. OpenRocket was used to analyze the drag coefficient when the active drag system was disengaged and is shown as a function of velocity in Figure 11 and as a function of time in Figure 13. The custom simulation was used to analyze the drag coefficient when the active drag was in use and is shown likewise as both a function of velocity, Figure 12, and a function of time, Figure 14.

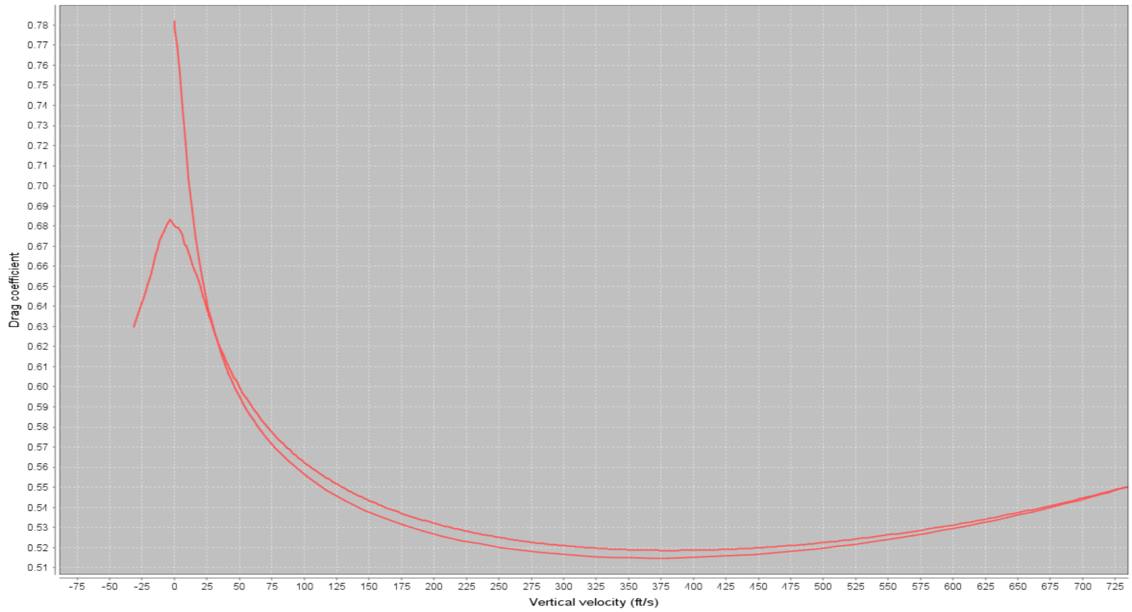

Figure 11. Coefficient of Drag Relative to Velocity with Active Drag Disengaged from OpenRocket

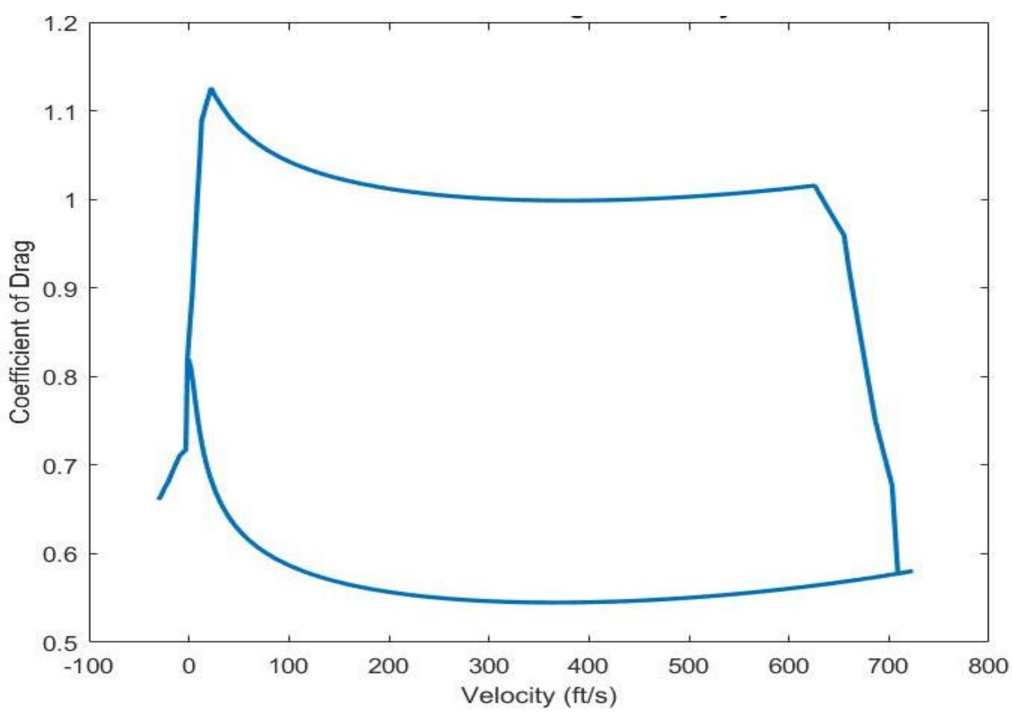

Figure 12. Custom Simulation of Coefficient of Drag Relative to Velocity with Active Drag Engaged

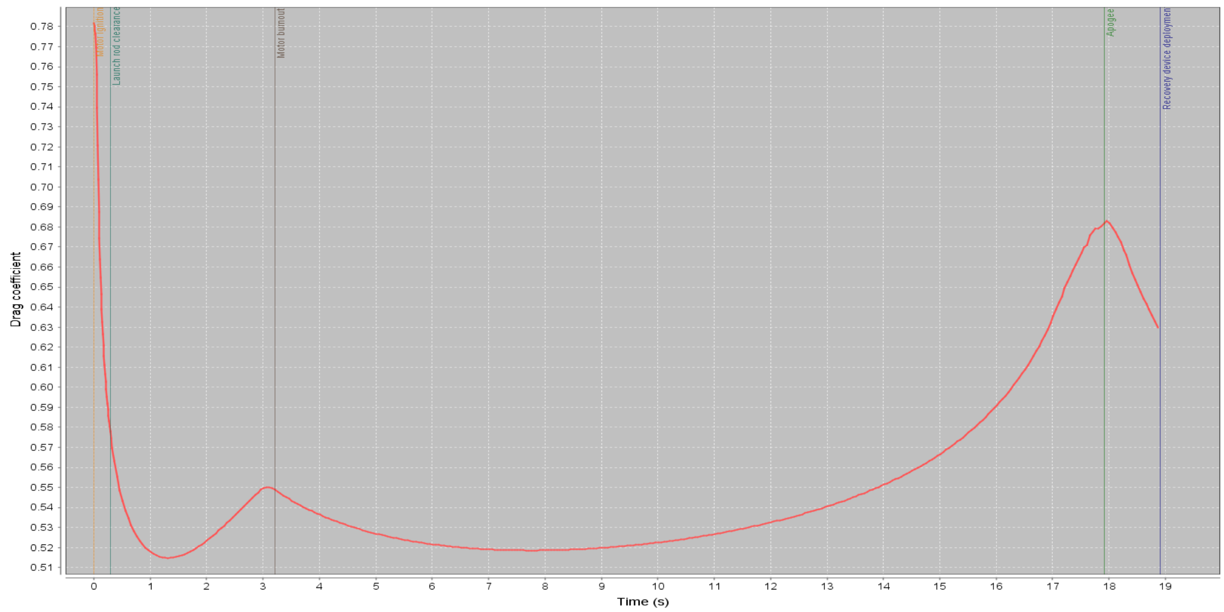

Figure 13. OpenRocket Coefficient of Drag, Active Drag Disengaged

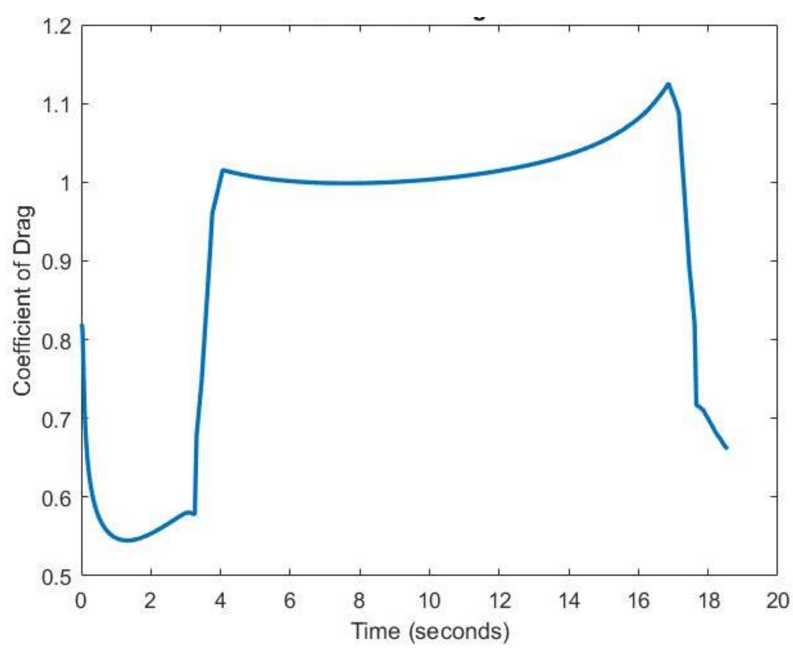

Figure 14. Custom Simulation Coefficient of Drag, Active Drag Engaged

2.3 Recovery Analysis

In addition to the OpenRocket simulation data, terminal velocity calculations were completed by hand. The terminal velocity is calculated as

$$V_T = \sqrt{\frac{2mg}{\rho A C_d}} \tag{2}$$

in which V_T is the parachute's terminal velocity, m is the mass of the components descending under the parachute, g is gravity, ρ is the air density, A is the frontal area, and C_d is the drag coefficient.

Using Equation 2, the terminal velocity of both the main and drogue parachutes are calculated. For the drogue calculation, the mass is found to be 11.108 lbm after subtracting the propellant, shock cord, and drogue parachute masses from the total mass. The terminal velocity after deployment of the drogue parachute is 72.0214 ft/s. For the main parachute calculation, the mass is found to be 10.723 lbm, which is the mass used for the drogue calculation minus the mass of the main parachute and shock cord. Using this mass, the terminal velocity after deployment of the main parachute is found to be 19.969 ft/s. This calculated velocity is acceptable as it is less than the maximum allowed descent rate of 24 ft/s.

It is also important that the vehicle does not descend too slowly as it will increase the drift distances and make retrieving the vehicle more difficult. All calculated values prove that our vehicle will be within range of safe decent speeds and will ease recovery of the vehicle post-launch. The plot of drift distance as a function of time for our vehicle can be seen in Figures 15 and 16. With our calculated descent velocities and predicted wind velocities, the vehicle's maximum drift is within reasonable distances.

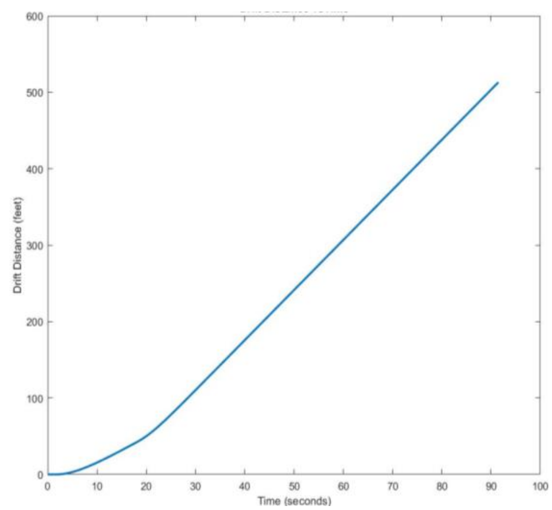

Figure 15. Custom Simulation of Drift Distance, Active Drag Disengaged

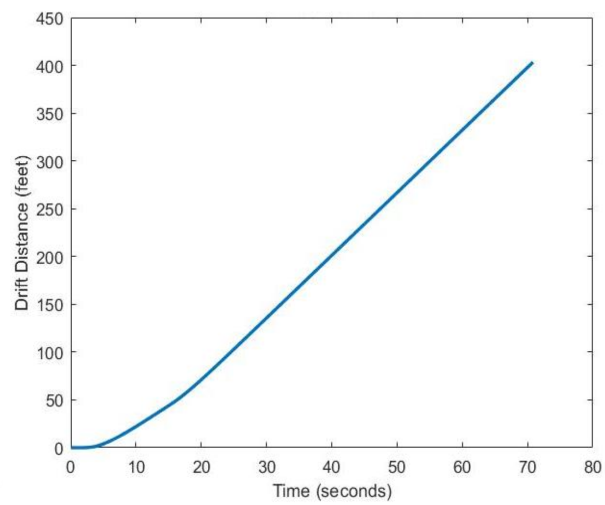

Figure 16. Custom Simulation of Drift Distance, Active Drag Engaged

2.4 Stability Analysis

OpenRocket was used to simulate stability margin caliber for the flight when the active drag is stowed. The lowest stability margin is 1.96 and occurs at launch rail clearance at 0.29 s. This is still well above the minimum stability margin of 1.00 to fly safely. The highest stability margin is 3.13 and occurs at motor burnout. This stability margin is well below the maximum stability margin of 5 required for safe flight. After motor burnout the stability margin slowly decreases, until a sharp drop near apogee, where the stability margin drops to 1.1. This phenomenon is most likely a result of a discontinuity in the simulation, not the physical features of the rocket, and therefore not likely an accurate prediction for stability near to apogee. There is also a sharp spike up to a stability margin of 3.46 at 5.85 s, which is also likely accounted for by a discontinuity in the simulation, and is likely not an accurate value of the stability at that time. The values of the stability margin throughout the flight can be seen in Figure 17.

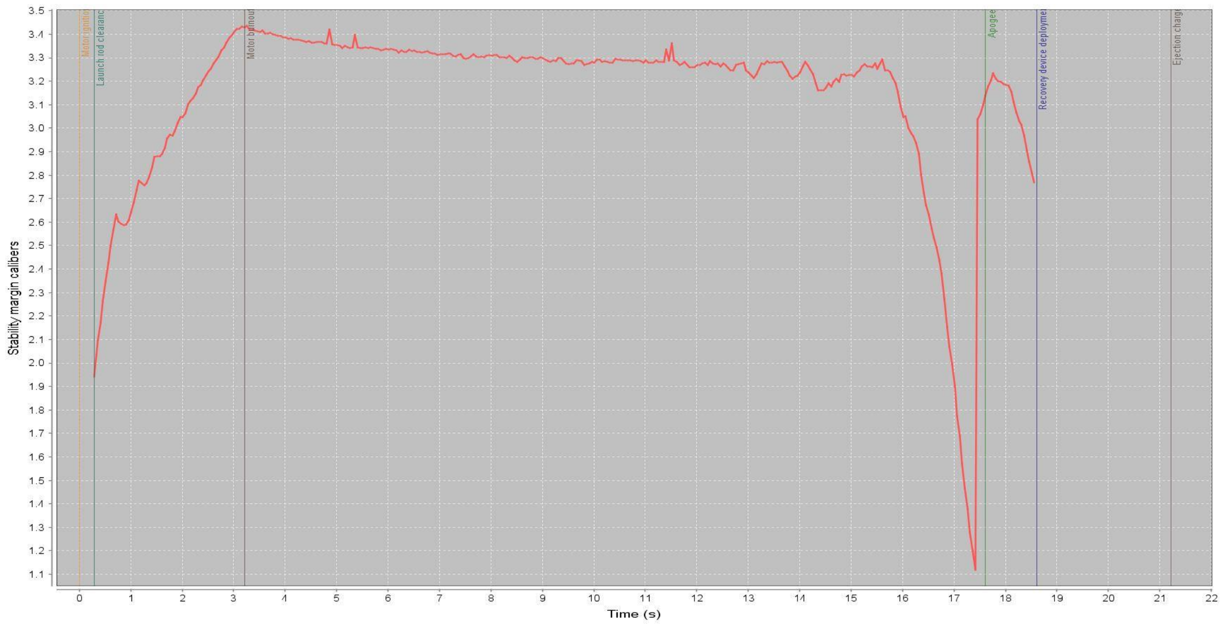

Figure 17. Stability Margin Calibers from OpenRocket

2.5 Environmental Conditions Analysis

When predicting the performance of the rocket prior to this point, a wind speed of 4.5 mph with 10% turbulence intensity in a direction perpendicular to vertical has been used in the simulations. Actual launch conditions will vary from the environmental conditions used in the simulation, either favorably or unfavorably. OpenRocket was used to simulate a 15 mph wind, which would be a high wind speed for launch, to ensure flight is still safe. With 15 mph wind, the rocket will drift 1746.66 ft, which is not too large a distance for drift given high wind speeds. The evenness of the launch site could pose the risk of not launching vertically. The team will check the evenness of the ground before launching and check the angle of the rocket on the launch rail with a level to verify that the rocket will launch in the desired direction.

The effect of the rocket on the environment must also be considered and precautions must be taken to minimize any potential damage. Starting at launch, it is possible that the heat or exhaust from the motor could damage the ground. This can be mitigated by ensuring that there is either an adequate blast shield in place. Another risk is that the rocket lands hard and damages the ground on impact. The team has taken this risk into account during design and has made sure that the descent rate is well below any speeds that would cause damage to either the ground or the rocket. If parts were to come loose during landing or take off and were left there, it would be damaging to environment. The team will check the rocket after recovery for any missing parts, and those missing parts (if there are any) will be located and removed.

3. Innovation

The active drag design is a unique design created to meet the competition requirements while minimizing cost and maximizing reliability, repeatability, and performance. The system made use of a small linear actuator in conjunction with spur gears, as noted in Sections 1.3.1 and 1.4, in a creative way to obtain a solution to the competition challenge requiring teams to create an active drag system that could cause the rocket to decrease maximum altitude to 75% of the initial maximum. All components included in both the rocket and active drag play key parts in the success of the flight, and are therefore integral to completing the challenge set forth by the competition.

4. Safety

4.1 Flight and Recovery Safety

The rocket has been designed with safety in mind for the entire flight and for recovery. During launch, the speed of the rocket at 6 ft up the rail exceeds the minimum requirement significantly, and the exit velocity off the rail exceeds the standard minimum exit velocity to ensure the rocket flight is vertical. The rocket has been designed such that the stability margin is an acceptable value for stable flight throughout the entire flight. The parachutes will be deployed at optimal times to ensure the landing speed is safely under 24 ft/s. To ensure ease of locating the rocket after flight, a GPS tracker will be used to obtain the exact landing location of the rocket.

4.2 Material-Handling Procedures

During construction, testing, and flight of the rocket, team members will be handling hazardous materials such as the flammable motor, epoxy, black powder charges, and fiberglass. At least one team member has experiences with each of these hazardous materials. The team member(s) with experience in the handling procedures will teach the other team members the proper techniques. Flammable materials will always be handled according to their instructions, keeping any possible flame source out of the range of the flammable materials and a fire extinguisher on hand in case of emergency. For handling epoxy and other possible skin irritants gloves will be worn at all times when contact is possible and drying pieces will be labelled as such to avoid anyone unknowingly coming into contact with epoxy. Black powder will be stored safely with all necessary precautions and will be measured precisely. Fiberglass will be handled with gloves to ensure that no fiber splinters are obtained as well as masks during cutting to avoid inhalation of fumes.

4.3 Assembly Procedures

Since assembly during the competition will be under time constraint, it is vital that all members of the team know how to assemble to rocket prior to the competition so that no mistakes are made that could compromise safety. Before the competition the team will go over the assembly slowly ensuring that all steps are carefully explained, and practice assembling the rocket until it can easily be done without mistakes in under one hour. Prior to assembly a checklist will be made with all the steps and parts to use during assembly as a guide to make sure nothing was left out or forgotten and to make sure all assembly steps are performed in the right order. The team will practice assembly enough times that such a checklist would not be required for assembly, but there as a safety. Additionally, each person involved in assembly will have specific tasks assigned to them to streamline the process, but all team members will be able to assemble the whole rocket in case of absence of one or more team members.

4.4 Pre- and Post-Launch Procedures

Prior to and after the launch of the rocket, team members will use precaution and follow predetermined procedures and safety codes. The team will first take inventory of all components to ensure that everything is there. The team will then begin assembling the rocket, being careful that all components are safely secured and in the proper position. The team will then survey the launch area and take into account any unevenness in the ground to ensure the rocket flies vertically. After the launch the team will first make sure the launch area is clear and it is safe to begin recovery. The GPS tracker in the rocket will be used to find the location of the rocket. Once the rocket is retrieved the landing site will be surveyed to check for any parts that may have come loose on impact. Once all parts have been recovered the team will make their way back to the setup area and begin the process again for the second flight.

5. Test Flights

5.1 Model Rocket Demonstration Flight

The model rocket was flown on November 7, 2015 at a Central Illinois Aerospace launch site in Monticello, IL. Figure 18 shows the process of preparing the rocket for launch on the launch rail. Figure 19 shows the team with the rocket post launch. This flight demonstrated that the team is capable of building, assembling, successfully launching and recovering a rocket.

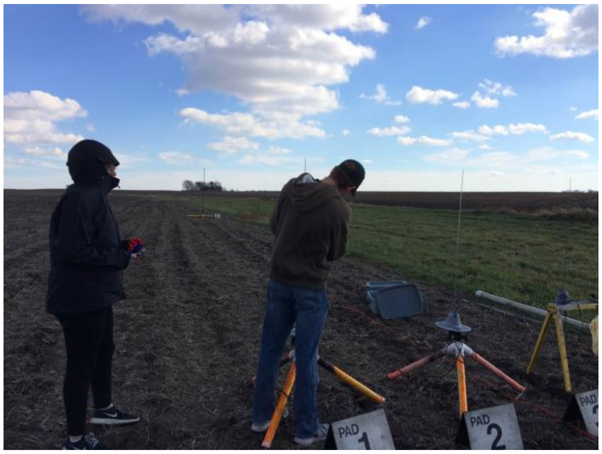

Figure 18. Launch Preparation

Figure 19. Model Rocket Pre-Launch

5.2 Test Flight Plan

The test flight will take place on April 23, 2016 at Rantoul Aviation Center through Central Illinois Aerospace. The rocket will be launched once, with the active drag utilized during flight. The motor used will be the Cesaroni K500, which is the same as the competition motor, and all competition avionics will be in place so as to best simulate competition conditions during the test flight. During this test flight the team will also practice assembling the rocket in under one hour as required on competition day. The results from the test flight will be compared to the simulations to see how close the apogee with the active drag engaged is to 75% of the apogee with the active drag disengaged. Analyzing these values will allow the team to make any changes needed to the active drag system to increase its performance before the competition date.

6. Budget

The project budget can be seen below in Table 3. The budget includes all parts that were purchased, the competition registration fee, and the estimated travel costs of the competition. In travel costs, it was assumed that team members would pay for their own food, so those costs were not taken into account in the team budget.

Table 3. Women in Aerospace Space Grant Team Planned Budget.

Eyebolts	$15.76
4" Blue Tube Coupler	$21.90
Blue Tube 4" diameter	$77.90
Nose Cone	$21.95
K500	$225.90
Motor Case	$84.69
Linear actuators	$108.99
12V Battery	$29.99
Actuator controller	$13.82
Fiberglass for fins	$51.42
Shock cords	$25.00
1/4" threaded rod	$13.44
1/4" nuts for threaded rod	$4.74
Camera	$8.19
Arduino	$9.89
Accelerometer	$13.99
Balsa wood block (for shroud)	$13.80
Paint (Pink)	$7.76
Paint (Silver)	$11.36
Plywood for sled	$3.99
Micro SD adapter for camera	$5.59
Quick Links	$5.40
Terminal Blocks	$9.75
9V Battery	$8.00
Battery Leads	$3.24
Blue Tube motor mount	$23.95
54mm Motor Retainer	$31.03
Rotary Switch	$28.38
Epoxy	$44.99
Epoxy Pumps	$12.99
Bulkheads	$16.20
Centering Rings	$16.20
1515 Rail Buttons	$4.43

Gear Rack	**$25.39**
Spur Gear	**$45.64**
Shear Pins	**$8.85**
Aluminum Rods	**$5.02**
Mirrors	**$2.99**
Registration Fee	**$400.00**
Travel Costs	**$1000.00**
Total Project Cost	**$2471.52**